



OPEN

Atomic Structures of Silicene Layers Grown on Ag(111): Scanning Tunneling Microscopy and Noncontact Atomic Force Microscopy Observations

Andrea Resta¹, Thomas Leoni¹, Clemens Barth¹, Alain Ranguis¹, Conrad Becker¹, Thomas Bruhn², Patrick Vogt² & Guy Le Lay¹

¹Aix-Marseille Université, CNRS, CINaM UMR 7325, 13288 Marseille, France, ²Technische Universität Berlin, Institut für Festkörperphysik, Hardenbergstrasse 36, 10623 Berlin, Germany.

Received
7 May 2013

Accepted
24 July 2013

Published
9 August 2013

Correspondence and
requests for materials
should be addressed to
A.R. (resta@cinam.
univ-mrs.fr)

Silicene, the considered equivalent of graphene for silicon, has been recently synthesized on Ag(111) surfaces. Following the tremendous success of graphene, silicene might further widen the horizon of two-dimensional materials with new allotropes artificially created. Due to stronger spin-orbit coupling, lower group symmetry and different chemistry compared to graphene, silicene presents many new interesting features. Here, we focus on very important aspects of silicene layers on Ag(111): First, we present scanning tunneling microscopy (STM) and non-contact Atomic Force Microscopy (nc-AFM) observations of the major structures of single layer and bi-layer silicene in epitaxy with Ag(111). For the (3×3) reconstructed first silicene layer nc-AFM represents the same lateral arrangement of silicene atoms as STM and therefore provides a timely experimental confirmation of the current picture of the atomic silicene structure. Furthermore, both nc-AFM and STM give a unifying interpretation of the second layer $(\sqrt{3} \times \sqrt{3})R \pm 30^\circ$ structure. Finally, we give support to the conjectured possible existence of less stable, $\sim 2\%$ stressed, $(\sqrt{7} \times \sqrt{7})R \pm 19.1^\circ$ rotated silicene domains in the first layer.

Silicene¹, a honeycomb arrangement of silicon atoms forming a new synthetic atom-thin two dimensional hexagonal silicon allotrope, has recently generated a very strong interest². It was first synthesized by silicon deposition onto silver (111) substrates¹⁻⁴ and further obtained by silicon segregation on top of zirconium diboride (0001) thin films grown on Si(111) templates⁵ and then recently by silicon deposition onto iridium (111) surfaces⁶. So far, STM combined with Scanning Tunneling Spectroscopy (STS) has played a key role in the characterization of this novel material, from the observation of different phases⁷ to signatures of a possible superconducting gap⁸. Although STM allows imaging surfaces with atomic resolution there is nevertheless sometimes some ambiguity in the interpretation of the observations. Since more than 10 years, nc-AFM has proven to be extremely powerful because it permits obtaining the same quality of true atomic resolution on any clean and atomically flat surface, even if the surface is insulating^{9,10}. In particular for conducting surfaces, STM and nc-AFM allow obtaining a complete set of information about electronic and geometric properties of surfaces¹¹ and molecules¹²⁻¹⁴. Such types of experiments strongly motivate to conduct nc-AFM experiments also on epitaxial silicene films, for assisting an accurate determination of the silicene structure and of its electronic properties.

Here, we present STM and nc-AFM results concerning the major silicene phases. We first examine the archetype (3×3) single layer silicene phase often referred as 4×4 phase with respect to the Ag(111) substrate^{4,15,16}. We focus on this phase since other first layer structures have not yet passed the two required criteria to be eligible to silicene, namely, a honeycomb atomic structure as well as signatures of π^* and/or π like states. Beyond the first layer, a new $(\sqrt{3} \times \sqrt{3})R \pm 30^\circ$ silicene phase (Ag(111) $(4/\sqrt{3} \times 4/\sqrt{3})R \pm 30^\circ$) superstructure with respect to Ag(111) as noted in reference 7 is identified at the next layer^{7,17} and even higher successive levels (Vogt, P. *et al.* Synthesis of graphitic silicon by multi-layer stacking of silicene. Manuscript in preparation.). In our experimental conditions, a comparison of the layer heights derived from nc-AFM and STM measurements assigns this structure to a new silicene phase¹⁷ (Vogt, P. *et al.* Synthesis of graphitic silicon by multi-layer stacking of silicene. Manuscript in preparation.), whose potential existence has been theoretically predicted some time



ago¹⁸ and recently explored in more detail^{19,20}. In contrast to previous assignments by Wu *et al.*^{21–23}, we have never observed the $(\sqrt{3} \times \sqrt{3})R \pm 30^\circ$ silicene phase as a first layer in direct contact with the Ag(111) surface in either nc-AFM or STM experiments at room temperature (RT) or at 77K. Despite this discrepancy, the present work confirms and emphasizes the major importance of this phase in the second layer.

Finally, the observation of rotational domains in the first layer gives a strong hint to the presence of less dense, $(\sqrt{7} \times \sqrt{7})R \pm 19.1^\circ$ silicene structures ($\sim 2\%$ tensile stress) in coincidence with Ag(111) $(\sqrt{13} \times \sqrt{13})R \pm 13.9^\circ$ supercells, as proposed in recent DFT calculations¹⁶. This should help interpreting the first Raman spectra of silicene acquired ex-situ on encapsulated multi-phase samples²⁴.

Results

Atomic scale contrast of STM and nc-AFM images. A high resolution STM image of the silicene (3×3) structure is shown in Fig. 1(a). The image was acquired at room temperature with a standard (non-oscillating) STM tip and shows main atomic details as previously observed in other STM experiments^{1,3,4}. In Fig. 1(b) we show for direct comparison an image obtained at the same scale by nc-AFM at 77K, which was recorded in the constant Δf mode. Both images and others (see supporting information) show typical atomic scale contrast features with a quite similar flower pattern. The most important observation is that the exact same number of perfectly symmetric bright dots or disks can be found within the unit cell of the structure at exactly same in-plane positions.

The structural model for the silicene film derived in reference 1 was developed by complementary STM and photoelectron spectroscopy measurements and assisting DFT calculations. This work addressed the bright features visible in Fig. 1 (a) to the atoms of the surface, which then gets a strong, timely support from also our nc-AFM data. Indeed, for perfect symmetric tips and well-chosen scanning parameters nc-AFM on silicon surfaces has been found to fairly well represent the true positions of surface atoms as often demonstrated on, e.g., the Si(111) (7×7) ^{25,26} or Si(001) surface²⁷.

Note that we clearly stress at this point that STM and nc-AFM images can not be quantitatively compared with each other: STM measures the tunnel current and nc-AFM the tip-surface force. Furthermore, the atomic scale contrast strongly depends on many parameters like the tip chemistry and structure^{26,27}, or on the tip-surface distance^{26,11}, which is generally not precisely known as it was the case for each of the two measurements shown in Fig. 1. All this may lead to differences in the atomic scale contrast, which can be seen for instance in Fig. 1 by comparing the profiles (c) of each image.

DFT calculations indicate that the bonds in first layer epitaxial silicene on Ag(111) surfaces should be of a mixed sp^2/sp^3 character^{1,3}. However, photoelectron spectroscopy measurements showing linear dispersions of π states for the silicene (3×3) silicene structure, as well as quantum interference pattern observations in low temperature scanning tunneling empty state imaging of the silicene $(\sqrt{3} \times \sqrt{3})R \pm 30^\circ$ have given compelling evidence of metallicity and of the presence of Dirac fermions with a very high Fermi velocity of $\sim 1.3/1.2 \cdot 10^6 \text{ ms}^{-1}$ in π/π^* states^{1,22}. In reference 22 the $(\sqrt{3} \times \sqrt{3})R \pm 30^\circ$ structure was considered a first layer structure, which is not in agreement with our observations demonstrating it as a 2nd, 3rd, etc. layer (Vogt, P. *et al.* Synthesis of graphitic silicon by multi-layer stacking of silicene. Manuscript in preparation.), however the reported properties are still valid. From our experiences with the nc-AFM imaging of the silicene film we can state that it is generally quite difficult to obtain the atomic scale contrast on the silicene film. Furthermore, if an atomic contrast is obtained, the contrast is relatively weak, particularly in comparison to the strong atomic contrast that can be regularly measured on the Si(111) (7×7) ²⁵ or Si(001)²⁷ surface. We believe that this might be a consequence of the sp^2/sp^3 character of the Si atoms within the silicene layer, which makes it different from the Si(111) surface with its pure sp^3 dangling bonds protruding from the Si atoms.

Other STM and nc-AFM experiments point in this direction, too: we could record the detuning (Δf) while regulating the tip-surface distance on the tunnel current, and, vice versa, record the tunnel current while regulating the tip-surface distance on the detuning Δf . In Fig. 2: image (a) is the atomic resolution topography image, which was obtained during the regulation on the tunneling current,

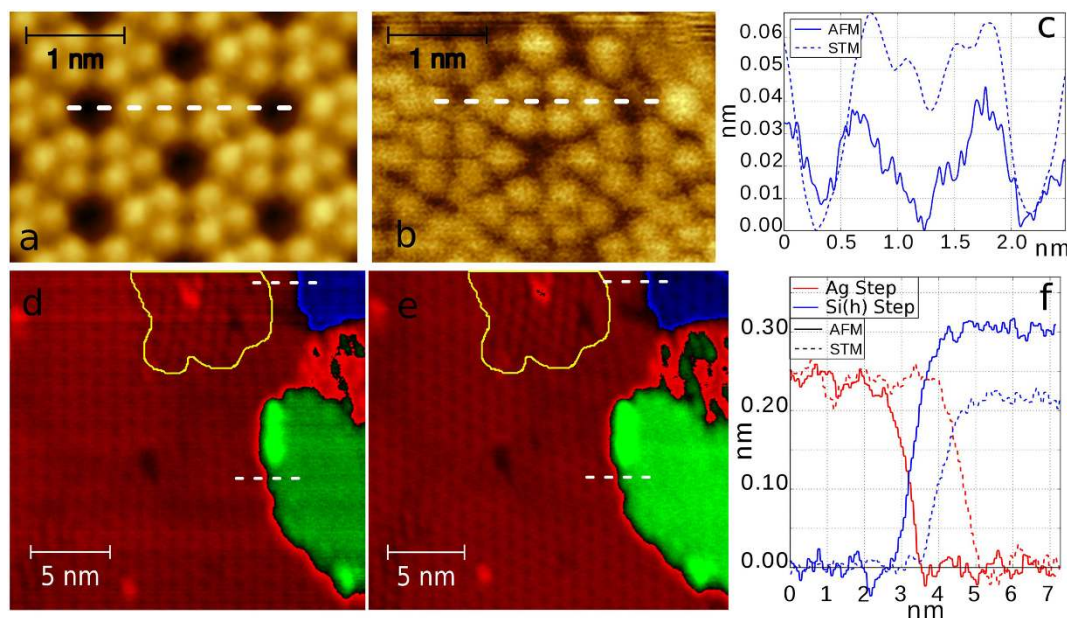


Figure 1 | (a) The (3×3) silicene reconstruction: STM imaging with a non oscillating tip (filled states, $U_{bias} = -1.13 \text{ V}$, $I = 0.53 \text{ nA}$). (b) nc-AFM image ($\Delta f = -1.0 \text{ Hz}$; $A_p-p = 4.5 \text{ nm}$, $f_0 = 26150 \text{ Hz}$). (c) Profiles along the dashed lines in image (a) and (b). (d) STM large scale image (filled states, $U_{bias} = -0.80 \text{ V}$, $I = 0.10 \text{ nA}$). (e) nc-AFM image of the same area ($\Delta f = -0.99 \text{ Hz}$; $A_p-p = 7.5 \text{ nm}$). (f) Profiles along the white dashed lines in image (d) and (e), calibrated accordingly to the Ag(111) step height of 0.236 nm.

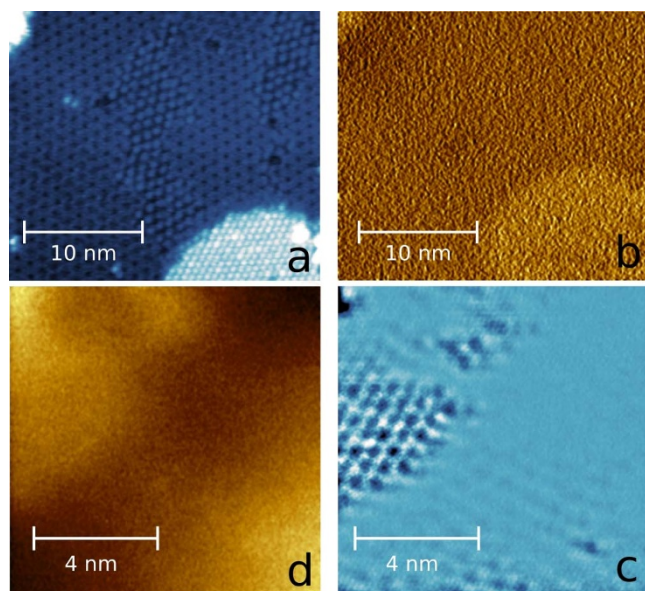


Figure 2 | (a) Topography image recorded at 77K during STM regulation on the current (filled states, $U_{\text{bias}} = -0.97$ V, $I = 0.2$ nA). (b) Corresponding Δf image recorded while regulating on the tunnel current ($A_{\text{p-p}} = 7.5$ nm). (c) Topography image recorded at 77K during constant Δf regulation ($\Delta f = -6.44$ Hz, $A_{\text{p-p}} = 4.5$ nm). (d) Corresponding current image recorded while regulating on Δf with an applied voltage of $U_{\text{bias}} = 0.08$ V.

image (b) shows variation of the detuning Δf , which was simultaneously recorded. The Δf image in Fig. 2 (b) does not bring any details compared to the topography image of the tunneling current – a normal situation when imaging silicene. Figure 2(c) shows a nc-AFM topography image, which was obtained during regulating on the detuning Δf whereas at the same time the tunneling current was recorded (d). The topography of the sample is hardly visible without any signs of atomic resolution, whereas on the contrary the simultaneously recorded tunneling current (d) reveals a clear atomic contrast in the same area. From both measurements (pure STM and nc-AFM) one can deduce that for obtaining atomic resolution on this system the tip has to be brought much closer to the surface during imaging in the nc-AFM mode than in the STM mode. In comparison, imaging the Si(111)(7×7) surface^{25,26} almost always leads to a clear atomic scale contrast in both channels, current and detuning Δf . Although the atomic resolution is first obtained in the STM current channel when approaching the tip to the Si(111)(7×7) surface it relatively quickly appears also in the detuning channel. This is in particular due to the strong chemical interaction between the last tip atom and the dangling bonds of the Si ad-atoms²⁶. We anticipate that the latter type of tip-surface interaction cannot be considered for our case, which explains the faint atomic contrast we always observe in our nc-AFM images. This agrees well with our previous results, assuming a mixed sp^2/sp^3 character for the single atoms within the silicene layer¹. This means that the silicene Si atoms differ significantly in terms of their electronic properties from those in the Si(111)(7×7) surface, resulting in a weaker tip-surface interaction. To shed more light onto the aspects of atomic contrast formation in STM and nc-AFM and the orbitals of the silicene film, the atomic scale contrast of experimental images needs to be compared with the one of images from theory, which have to model realistic tips with different structures and chemistries as exemplified in, e.g., reference 26.

Second silicene layer. STM and nc-AFM images with a larger scale consecutively acquired at 77K in the same area are displayed in Fig. 1(d) and (e). The STM image was obtained while regulating

the tip-surface distance on the tunnel current with the oscillating Q-plus sensor whereas the nc-AFM image was obtained in the pure contrast Δf topography mode with a bias at the tip (current images: see supporting information). The two images appear remarkably similar and exhibit the silicene(3×3) structure as the dominant domain, on the large terrace (red). In the region surrounded by the yellow line another domain can be seen, which is tentatively attributed to a $\text{Ag}(111)(\sqrt{13} \times \sqrt{13})R \pm 13.9^\circ$ superstructure in relation to its orientation and cell size. A lower terrace (blue) is visible at the top right corner of each image. There, the same (3×3) silicene structure ($\text{Ag}(111)(4 \times 4)$) as on the large terrace (red) can be seen (see also supporting information). The height difference between the two regions, as measured from the profiles in Fig. 1(f), equals the height of a monoatomic Ag(111) step (0.236 nm). These two regions are in fact two distinct silver terraces, each one covered by the silicene(3×3) layer.

An interesting observation in Fig. 1(d) and (e) is the island, which exhibits no atomic contrast at all, on the right side in each image (green). In fact, it is a general feature of the surface often observed in other STM and nc-AFM images (see supporting information). In the STM image the height of this island with respect to the adjacent surface region (red) is about 0.22 nm, which is slightly lower than the height of a single silver step, while it is higher in the nc-AFM image (0.30 nm). Such an island cannot be a nanometer sized silver ad-island since none was ever observed on the bare silver surface. Although the structure of the island is, so far, not identified we provisionally assume that it is the second silicene($\sqrt{3} \times \sqrt{3})R \pm 30^\circ$ layer (see below). We underline here that whether imaging at room temperature or at ~ 77 K, as in the present case, we have never observed the presence of silicene($\sqrt{3} \times \sqrt{3})R \pm 30^\circ$ domains directly on the Ag(111) surface. This is at variance with the situation described in references 21 and 22, where the silicene($\sqrt{3} \times \sqrt{3})R \pm 30^\circ$ reconstruction is attributed to the very first silicene layer. In contrast, our observations are in perfect agreement with recently published observations²⁸.

An example where we could obtain true atomic resolution on the second silicene layer is shown in Figure 3. Image (a) shows an atomically resolved STM image obtained at 77 K using the Qplus sensor in the pure STM mode on a ($\sqrt{3} \times \sqrt{3})R \pm 30^\circ$ reconstructed second layer silicene island, 0.22 nm in height. The image results from a double tip, which produced two interesting and important types of contrasts, previously observed by other groups: a honeycomb arrangement, as previously reported in references¹⁷ (Vogt, P. *et al.* Synthesis of graphitic silicon by multi-layer stacking of silicene. Manuscript in preparation.) and a hexagonal array of protrusions, as reported in reference 7. Since one and the same island was imaged

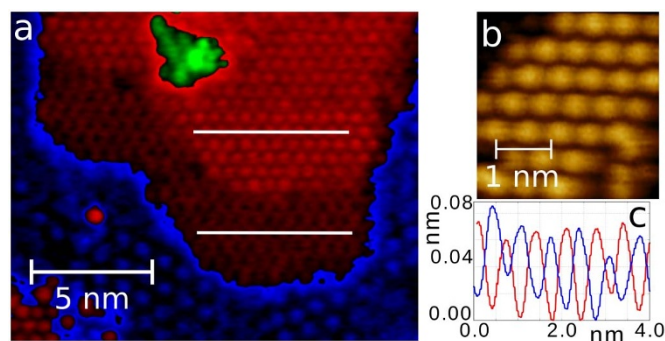


Figure 3 | Two different contrasts originating from a double tip with two different chemical apexes observed upon imaging the second silicene layer. (a) STM topography image (filled states, $U_{\text{bias}} = -0.4$ V, $I = 0.1$ nA). (b) The second layer of silicene, nc-AFM topography image ($\Delta f = -4.1$ Hz, $A_{\text{p-p}} = 7.5$ nm), (c) Line profiles red/blue corresponding to the two upper/lower white lines in image (a).



by both distinct sub-tips, both types of contrasts result from the same, unique, $(\sqrt{3} \times \sqrt{3})R \pm 30^\circ$ silicene structure. Most likely, the apexes of the two tips have different terminations, one terminated with, e.g., a W atom and the other one with a Si atom, which generates different atomic contrasts, as already reported for other systems²⁹. Figure 3(b) shows a zoom-in of the second layer island taken in nc-AFM mode, imaged as a hexagonal array of protrusions. Figure 3(c) shows the profiles measured along the parallel white lines in the STM image of the second layer island of Fig. 3(a), they agree in the periodicity and corrugation of the atomic structure. We can therefore conclude at this point that the silicene $(\sqrt{3} \times \sqrt{3})R \pm 30^\circ$ structure can appear, depending on tip conditions, either as a honeycomb arrangement or a complimentary hexagonal array of protrusions, thus conciliating apparently adverse previous observations^{17,21,23}.

Domains in silicene films. In addition to the 4×4 silver superstructure, which corresponds to the most stable 3×3 silicene phase according to DFT calculations (reference 16 and private communication), other $(\sqrt{13} \times \sqrt{13})R \pm 13.9^\circ$ superstructures with respect to the silver substrate can also be observed in the first layer, as exemplified in Figs. 1 and 2 (see also supporting information). For these minority superstructures, different silicene reconstruction models have been proposed through DFT calculations, e.g., in references 3,5. However, the most likely appears to be a structure where rotated $(\sqrt{7} \times \sqrt{7})R \pm 19.1^\circ$ silicene domains would match each of the two $(\sqrt{13} \times \sqrt{13})R \pm 13.9^\circ$ Ag(111) supercells (see reference 16). Such domains would be less stable (-0.332 eV per Si atom versus -0.368 eV), being inherently in tensile stress ($\sim 2\%$ in-plane stress) with respect to the 3×3 ground state silicene phase, while containing $\sim 4\%$ less silicon atoms per unit area. The STM measurements presented in Fig. 4 give a timely strong support to this interpretation.

Figure 4 contains four domains generated by the two symmetric domains of the silicene $(\sqrt{7} \times \sqrt{7})R \pm 19.1^\circ$ reconstruction in coincidence with the two symmetric Ag(111) $(\sqrt{13} \times \sqrt{13})R \pm 13.9^\circ$ supercells. As mentioned before, each of the two silver superstructures may comprise two silicene domains; this leads to four possible

silicene domains defined by the combination of the rotation angles: a) $+19.1^\circ/+13.9^\circ$; b) $+19.1^\circ/-13.9^\circ$; c) $-19.1^\circ/+13.9^\circ$ d) $-19.1^\circ/-13.9^\circ$. As can be seen in Fig. 4 these four domains can be grouped into two families in accordance with the angles between the Ag[10] surface unit vector and the silicene [10] one: $\pm 5.2^\circ$ or $\pm 33^\circ$. Each family produces a typical contrast. The first family appears as a hexagonal array of protrusions, whose rows are aligned at $\pm 5.2^\circ$ away from the Ag[10] surface vector. The second family, for which the silicene unit vector is rotated $\pm 33^\circ$ away from the Ag[10] surface vector, appears as a hexagonal moiré like pattern with the side of the hexagonal moiré at ± 13.9 degrees from the Ag[10] surface vector. Those two topographic aspects have been already imaged by STM in references 4 and 7, but not recognized as belonging to the same structure. Hence the recognition of four domains strongly supports the assumption of stressed, rotated silicene sheets, with most probably the same atomic structure, as typically inferred through DFT calculations by Gao and Zhao in reference 16.

Discussion

Summarizing, we have shown that STM and nc-AFM images with atomic resolution of the first layer of epitaxial silicene (3×3) films on Ag(111) show same atomic positions within the unit cell, despite the very different imaging mechanisms of both techniques. The image contrast is characterized by a unique flower pattern as we described in reference 1. Clearly, this similarity gives a timely further strong support for the structural model of epitaxial silicene we have proposed in reference 1. Furthermore, simultaneously acquired STM and nc-AFM images show an atomic contrast in preferentially the STM images. An atomic contrast in nc-AFM images can only be obtained if the tip is approached to the surface in very close distances. This finding can be explained by the π/π^* orbitals of the silicene film as compared, typically, to the sp^3 dangling bonds of the Si(111) surface.

By STM we have observed four different rotational domains in the first layer, coexisting with the majority (3×3) silicene phase. We can reduce the apparent complexity of the system upon recognizing that, despite their two aspects, the four domains stem from one and the same atomic structure. Our interpretation is that the two aspects result from the two equivalent silicene $(\sqrt{7} \times \sqrt{7})R \pm 19.1^\circ$ reconstructions

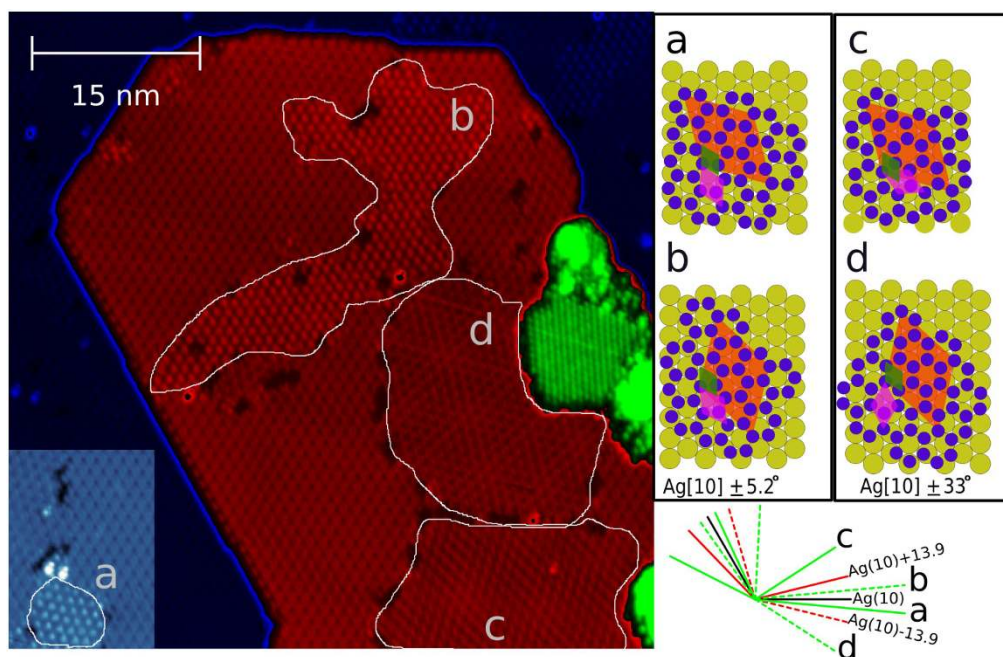


Figure 4 | (a) STM topography image acquired at room temperature with a non oscillating tip (filled states, $U_{bias} = -1.18$ V, $I = 0.33$ nA). (b) Ball model (silicon atoms are in blue, silver atoms in yellow) of the four distinct domains. The silicene $(\sqrt{7} \times \sqrt{7})R \pm 19.1^\circ$ unit cells in coincidence with the Ag(111) $(\sqrt{13} \times \sqrt{13})R \pm 13.9^\circ$ unit cells are in orange; the silicene 1×1 unit cells are in magenta and in green the Ag(111) 1×1 cells.



matching each of the two symmetrically equivalent domains of the $\text{Ag}(111)(\sqrt{13} \times \sqrt{13})R \pm 13.9^\circ$ superstructure, a point that has not been recognized before.

Finally, the combination of both STM and nc-AFM imaging techniques, allowed revealing the overgrowth of second layer silicene islands with a unique $(\sqrt{3} \times \sqrt{3})R \pm 30^\circ$ reconstruction, appearing at atomic resolution, either as a honeycomb arrangement or a complimentary hexagonal array of protrusions, depending on the tip apex termination.

Our results are a promising start for future developments and measurements, in particular in view of nc-AFM. For instance, three-dimensional force spectroscopy^{30,31} at low temperature in combination with theoretical calculations could be accomplished to understand the precise mechanism of the atomic contrast formation. If in the course of such experiments the bias voltage is varied as an additional parameter, very important electronic properties of the silicene films could be extracted as well, as it has been exemplified on the $\text{Si}(111)(7 \times 7)$ surface³². Such experiments could be further assisted by Kelvin probe microscopy³³, which has shown to be quite powerful for measuring, e.g., work function differences at the nanometer³⁴ and even atomic scale³⁵. Most importantly, since STM as well as nc-AFM nowadays allow manipulating atoms³⁶, molecules³⁷ and clusters³⁸, the two types of microscopes could be used, in principle, to manipulate the second layer silicene islands on the first one, provided that the coupling between the layers is only weak. Note that the manipulation of thin films has been exemplified by recent experiments of NaCl films on $\text{Cu}(111)$ ³⁹. Such achievements are very encouraging and open the way for manipulating silicene layers or possibly the exfoliation of monolayer sheets.

Methods

The room temperature STM experiments were done with an Omicron 1 STM whereas the low temperature experiments were carried out at $\sim 77\text{K}$ in an Omicron low temperature STM/AFM microscope hosted in an ultra-high vacuum chamber with a base pressure in the temperature. The atomic force microscope was operated in the frequency modulated non-contact mode^{9,10} using a quartz tuning fork (Q-plus³⁰) in a configuration that allows switching from STM to nc-AFM and vice-versa. In particular, it allowed acquiring consecutive images in either of the modes on exactly the same surface area. The resonance frequencies of the QPlus sensors, stabilized to an amplitude (A_{p-p}) of a few nanometers, were in the order of $f_0 = 26\text{kHz}$. Electrochemically etched tungsten tips were glued at the end of the free branch of the tuning fork such that it allowed the simultaneous acquisition of the detuning (Δf) and tunneling current (I). All nc-AFM images were obtained with an active distance feedback loop while regulating on a constant detuning Δf . During nc-AFM measurements the tip bias voltage was applied to the substrate, in general it was kept at zero Volt. Electrostatic force spectroscopy measurements (detuning (Δf) versus bias voltage (U_{bias}) curves) carried out on the sample surface revealed a contact potential difference between tip and surface lower than 0.08V , which indicates that long range electrostatic forces are negligible and do not need to be compensated by applying a bias voltage. The STM topographs were obtained by regulating the tunnel current with an active distance feedback loop. The tip was oscillating during the acquisition of the STM images with amplitude stabilized at a few nanometers. Note that two STM images (Fig. 1(a) and Fig. 4) were obtained at room temperature with an Omicron STM and a non-oscillating STM tip.

The $\text{Ag}(111)$ single crystal surface was cleaned by cycles of sputtering with argon ions and annealing at 500C° . Silicene, sublimated from a $\sim 3 \times 10\text{mm}^2$ piece of silicon wafer heated by direct current at $\sim 1100\text{C}^\circ$, was deposited at a rate below 0.05monolayer/min onto the clean $\text{Ag}(111)$ substrate kept at $\sim 230\text{C}^\circ$.

- Vogt, P. *et al.* Compelling Experimental Evidence for Graphenelike Two-Dimensional Silicon. *Phys. Rev. Lett.* **108**, 155501 (2012).
- Xu, M., Liang, T., Shi, M. & Cheng, H. Graphene-like two dimensional materials, *Chemical Reviews* **113**, 3766 (2013).
- Lin, C.-L. *et al.* Structure of Silicene Grown on $\text{Ag}(111)$. *Appl. Phys. Exp.* **5**, 045802 (2012).
- Chiappe, D., Grazianetti, C., Tallarida, G., Fanciulli, M. & Molle, A. Local Electronic Properties of Corrugated Silicene Phases. *Adv. Mater.* **24**, 5088 (2012).
- Fleurence, A. *et al.* Y. Experimental Evidence for Epitaxial Silicene on Diboride Thin Films. *Phys. Rev. Lett.* **108**, 245501 (2012).
- Meng, L. *et al.* Buckled Silicene Formation on $\text{Ir}(111)$. *Nano Lett.* **13**, 685 (2013).
- Arafune, R. *et al.* Structural transition of silicene on $\text{Ag}(111)$. *Surface Science* **608**, 297 (2013).
- Chen, L., Feng, B. & Wu, K. Observation of a possible superconducting gap in silicene on $\text{Ag}(111)$ Surface. *App. Phys. Lett.* **102**, 081602 (2013).

- Barth, C., Foster, A. S., Henry, C. R. & Shluger, A. L. Recent Trends in Surface Characterization and Chemistry with High-Resolution Scanning Force Methods. *Adv. Mater.* **23**, 477 (2011).
- Hofer, W. A., Foster, A. S. & Shluger, L. A. Theories of scanning probe microscopes at the atomic scale. *Rev. Mod. Phys.* **75**, 1287 (2003).
- Sweetman, A. *et al.* Simultaneous noncontact AFM and STM of $\text{Ag:Si}(111)-(\sqrt{3} \times \sqrt{3})R30^\circ$. *Phys. Rev. B* **87**, 075310 (2013).
- Gross, L., Mohn, F., Moll, N., Liljeroth, P. & Meyer, G. The Chemical Structure of a Molecule Resolved by Atomic Force Microscopy. *Science* **325**, 1110 (2009).
- Repp, J., Meyer, G., Paavilainen, S., Olsson, F. E. & Persson, M. Imaging Bond Formation Between a Gold Atom and Pentacene on an Insulating Surface. *Science* **312**, 1196 (2006).
- Guillermet, O. *et al.* STM and AFM high resolution intramolecular imaging of a single decastarphene molecule. *Chem. Phys. Lett.* **511**, 482 (2011).
- Le Lay, G., De Padova, P., Resta, A., Bruhn, T. & Vogt, P. Epitaxial silicene: can it be strongly strained? *J. Phys. D: Appl. Phys.* **45**, 392001 (2012).
- Gao, J. & Zhao, J. Initial geometries, interaction mechanism and high stability of silicene on $\text{Ag}(111)$. *Sci. Rep.* **2**, 1 (2012).
- De Padova, P. *et al.* Evidence of Dirac fermions in multilayer silicene. *Appl. Phys. Lett.* **102**, 163106 (2013).
- Takeda, K. & Shiraishi, K. Theoretical possibility of stage corrugation in Si and Ge analogs of graphite. *Phys. Rev. B* **50**, 14916 (1994).
- Kamal, C., Chakrabarti, A., Banerjee, A. & Deb, S. K. Silicene beyond mono-layers different stacking configurations and their properties. *J. Phys.:Condens. Matter* **25**, 085508 (2013).
- Motohiko, E. Quasi-Topological Insulator and Trigonal Warping in Gated Bilayer Silicene. *J. Phys. Soc. Japan* **81**, 104713 (2012).
- Feng, B. *et al.* Evidence of Silicene in Honeycomb Structures of Silicon on $\text{Ag}(111)$. *Nano Lett.* **12**, 3507 (2012).
- Chen, L. *et al.* Evidence for Dirac Fermions in a Honeycomb Lattice Based on Silicon. *Phys. Rev. Lett.* **109**, 056804 (2012).
- Chen, L. *et al.* Spontaneous Symmetry Breaking and Dynamic Phase Transition in Monolayer Silicene. *Phys. Rev. Lett.* **110**, 085504 (2013).
- Cinquanta, E. *et al.* Getting through the nature of silicene: sp²-sp³ two-dimensional silicon nanosheet. arXiv:1212.5422v3.
- Eguchi, T. & Hasegawa Y. High Resolution Atomic Force Microscopic Imaging of the $\text{Si}(111)7 \times 7$ Surface: Contribution of Short-Range Force to the Images. *Phys. Rev. Lett.* **89**, 266105 (2002).
- Pérez, R., Stíchl, I., Payne, M. C. & Terakura, K. Surface-tip interactions in noncontact atomic-force microscopy on reactive surfaces: $\text{Si}(111)$. *Phys. Rev. B* **58**, 10835 (1998).
- Sweetman, A., Jarvis, S., Danza, R. & Moriarty, P. Effect of the tip state during qPlus noncontact atomic force microscopy of $\text{Si}(100)$ at 5K: Probing the probe. *Beilstein J. Nanotechnol.* **3**, 25 (2012).
- Lin, C.-L. *et al.* Substrate-Induced Symmetry Breaking in Silicene. *Phys. Rev. Lett.* **110**, 076801 (2013).
- Calleja, F. *et al.* Contrast Reversal and Shape Changes of Atomic Adsorbates Measured with Scanning Tunneling Microscopy. *Phys. Rev. Lett.* **92**, 206101 (2004).
- Berger, J. *et al.* Characterization of the mechanical properties of qPlus sensors. *Beilstein J. of Nanotechnol.* **4**, 1 (2013).
- Sugimoto, Y., Namikawa, T., Miki, K., Abe, M. & Morita, S. Vertical and lateral force mapping on the $\text{Si}(111)-(7 \times 7)$ surface by dynamic force microscopy. *Phys. Rev. B* **77**, 195424 (2008).
- Arai, T. & Tomitori, M. Observation of Electronic States on $\text{Si}(111)-(7 \times 7)$ through Short-Range Attractive Force with Noncontact Atomic Force Spectroscopy. *Phys. Rev. Lett.* **93**, 256101 (2004).
- Melitz, W., Shen, J., Kummel, A. C. & Lee, S. Kelvin probe force microscopy and its application. *Surf. Sci. Rep.* **66**, 1 (2011).
- Cabailh, G., Henry, C. R. & Barth, C. Thin NaCl films on silver (001): island growth and work function. *New J. of Phys.* **14**, 103037 (2012).
- Sadewasser, *et al.* New Insights on Atomic-Resolution Frequency-Modulation Kelvin-Probe Force-Microscopy Imaging of Semiconductors, *Phys. Rev. Lett.* **103**, 266103 (2009).
- Oyabu, N., Custance, O., Yi, I., Sugawara, Y. & Morita, S. Mechanical Vertical Manipulation of Selected Single Atoms by Soft Nanoindentation Using Near Contact Atomic Force Microscopy. *Phys. Rev. Lett.* **90**, 176102 (2003). Sweetman, A. *et al.* Toggling Bistable Atoms via Mechanical Switching of Bond Angle. *Phys. Rev. Lett.* **106**, 136101 (2011).
- Leoni, T. *et al.* Controlling the Charge State of a Single Redox Molecular Switch. *Phys. Rev. Lett.* **106**, 216103 (2011).
- Hynninen, T., Cabailh, G., Foster, A. S. & Barth, C. Defect mediated manipulation of nanoclusters on an insulator. *Sci. Rep.* **3**, 1270 (2013).
- Bombis, Ch. *et al.* Mechanical Behavior of Nanocrystalline NaCl Islands on $\text{Cu}(111)$. *Phys. Rev. Lett.* **104**, 185502 (2010).

Acknowledgments

This work was supported by the “2D-NANOLATTICES” project of the Future and Emerging Technologies (FET) program within the 7th framework program for research of



the European Commission, under FET Grant No. 270749 and by the Deutsche Forschungsgemeinschaft (DFG) under Grant No. VO1261/3-1.

Author contributions

Resta A., Leoni T., Barth C., Vogt P., Bruhn T., Ranguis A. and Becker C. devised and performed the measurements conceived by Resta A., Vogt P., Barth C., Becker C. and Le Lay G. ; Resta A., Leoni T., Barth C. and Le Lay G. analyzed the data whereas Resta A., Barth C. and Le Lay G. wrote the article that was further discussed and finalized by all co-authors.

Additional information

Supplementary information accompanies this paper at <http://www.nature.com/scientificreports>

Competing financial interests: The authors declare no competing financial interests.

How to cite this article: Resta, A. *et al.* Atomic Structures of Silicene Layers Grown on Ag(111): Scanning Tunneling Microscopy and Noncontact Atomic Force Microscopy Observations. *Sci. Rep.* 3, 2399; DOI:10.1038/srep02399 (2013).



This work is licensed under a Creative Commons Attribution-NonCommercial-ShareAlike 3.0 Unported license. To view a copy of this license, visit <http://creativecommons.org/licenses/by-nc-sa/3.0>



SUBJECT AREAS:
STRUCTURE OF SOLIDS
AND LIQUIDS

SCANNING PROBE
MICROSCOPY

MATERIALS FOR DEVICES

SURFACES, INTERFACES AND
THIN FILMS

SCIENTIFIC REPORTS:

3 : 2399

DOI: 10.1038/srep02399
(2013)

Published:
9 August 2013

Updated:
20 November 2013

ERRATUM: Atomic Structures of Silicene Layers Grown on Ag(111): Scanning Tunneling Microscopy and Noncontact Atomic Force Microscopy Observations

Andrea Resta, Thomas Leoni, Clemens Barth, Alain Ranguis, Conrad Becker, Thomas Bruhn, Patrick Vogt & Guy Le Lay

This Article contains a typographical error in the Methods section.

“The room temperature STM experiments were done with an Omicron 1 STM whereas the low temperature experiments were carried out at ~ 77 K in an Omicron low temperature STM/AFM microscope hosted in an ultra-high vacuum chamber with a base pressure in the temperature.”

should read

“The room temperature STM experiments were done with an Omicron 1 STM whereas the low temperature experiments were carried out at ~ 77 K in an Omicron low temperature STM/AFM microscope hosted in an ultra-high vacuum chamber with a base pressure in the 10^{-11} mbar range. The sample and tips were cooled down to liquid nitrogen temperature.”